"Twin screw extrusion processing of double base rocket propellant"

Proceedings of AICHE Annual Meeting Austin, Texas

Processing and Safety of Energetics Materials Session

November 11, 2004

Suzanne Prickett*, William Newton*, Stuart Richman*, Wayne Thomas*, Christopher Gonzalez*, Dilhan Kalyon[•], Halil Gevgilili[•], Moinuddin Malik[••] Tugrulbey Kiryaman[••] and James E. Kowalczyk[••]

* Naval Surface Warfare Center

Indian Head Division

Indian Head, MD 20640-5035

[•] Highly Filled Materials Institute

Stevens Institute of Technology, Castle Point

Hoboken, NJ 07030

[••] Material Processing & Research, Inc.

31 Mercer St. 2-E

Hackensack, NJ 07601

ABSTRACT

Rocket propellants are generally manufactured using dated technologies, which involve batch mixing and ram extrusion. This paper outlines various tasks involved in the development of the twin screw extrusion process for the state-of-the-art manufacture of double base propellants. These tasks include TGA and DSC analysis, the characterization of various material functions including temperature and wall shear stress dependent shear viscosity, extrudate swell, flow instability and wall slip behavior of the propellant, the simulation of the coupled flow and heat transfer occurring in the twin screw extruder, the design of the die employing FEM calculations, and validation experiments using a thermal imaging camera and a well-instrumented twin screw extruder. Such characterization and simulation tasks are essential to the safe processing of energetic materials, which can be accomplished without the use of precarious trial-and-error procedures.

INTRODUCTION

The processing of rocket propellants generally uses dated technologies involving the batch mixing of the ingredients into sheet stock, followed by ram extrusion of the grains into the desired shape. In such batch processing the costs are relatively high and quality control issues are difficult to resolve. The use of the modern twin screw extrusion technologies has the potential of decreasing the labor/manufacturing costs, while at the same time improving the quality of the propellant.

Here some of these tasks, which were necessary in the development of a continuous processing technology for the manufacture of a double base propellant are outlined with some typical results. These tasks include: a) weld line healing studies, b) TGA and DSC analysis, c) the characterization of various material functions, including temperature and wall shear stress dependent shear viscosity, extrudate swell, flow instability and wall slip behavior of the propellant, d) the simulation of the coupled flow and heat transfer occurring in the twin screw extruder, e) the design of the die employing FEM calculations, and f) validation experiments using a thermal imaging camera and a well-instrumented twin screw extruder. Such characterization and simulation tasks are essential to the safe processing of energetic materials, which can be accomplished without the use of precarious trial-and-error procedures. In this paper only a portion of the experimental and simulation methodologies (sufficient to illustrate the overall concept and the methodology of the development) will be revealed.

The processing of the double base propellant in a twin screw extruder involves the steps of feeding the pellets of the formulation into the mixing volume of a twin screw extruder at the correct screw and barrel configuration, the coupled heat transfer and flow of the pellets within the mixing volume of the processor, and the pressurization of the suspension and shaping through a die. Thus, the propellant is subjected to a complex thermo-mechanical history in the extruder, necessitating that first one investigate what would happen to the stability of the propellant under such temperature, pressure and shearing conditions. Some of these characterization studies are described first.

TGA and DSC Studies:

The objective of the DSC and TGA experiments was to determine if there is a phase change or a reaction during the processing of the double base propellant (especially an auto-catalytic runaway decomposition reaction with fast kinetics) which would occur in the typical residence time and temperature conditions predicted for the twin screw extrusion process. The typical DSC scan shown in Figure 1 indicates that in the ambient to 105 °C (220°F) temperature range there are no significant endothermic or exothermic changes nor first or second order transitions, which could be picked up with DSC.

In the TGA experiment the specimen is subjected to various temperatures and the time-dependent weight of the specimen is determined under very precise conditions. Typical data are shown in Figure 2 at a temperature of 99°C (210 °F) along with the details of the conditions used. There is a linear decrease of the weight of the specimen with increasing time at 99°C (210 °F). The weight loss at the end of about 32 minutes is about 5.2% at the temperature of 99°C (210 ºF). It can be assumed that the moisture content of the specimens would be reduced while the temperature is being ramped up to the test temperature, thus the volatiles observed at relatively higher temperatures are other than moisture. It is not clear which ingredients of the double base formulation are being lost to give rise to the decrease in weight.

Let us now see the temperature dependent data (Figure 3). As shown the increasing temperature gives rise to a greater slope of weight change with time, suggesting a greater rate of decomposition. The slope change in the weight versus time behavior occurs at a temperature of 93°C (200°F). The weight loss can be kept within 2.5 % upon a duration of 30 minutes at temperatures less than and equal to 88°C (190 °F).

The ramifications of these findings on the twin screw extrusion process needed to be elucidated. It was important to review the cook off data of AA-2 propellant and the conditions under which the cook off tests are carried out and understanding of the temperature dependent weld line healing behavior. It was worthwhile to investigate further which components of the formulation are being lost and the behavior at temperatures other than those reported here. Overall, these results suggested caution for the continuous processing runs to take place and led to the decision to keep the temperature to be equal or less than 88°C (190°F).

Thermal conductivity of the propellant:

The temperature dependent values of the propellant are important to characterize. These data are necessary for mathematical modeling of the coupled flow and heat transfer occurring in the processor as well as providing additional input into the stability of the propellant at various temperatures. The thermal conductivity of the propellant was determined by subjecting the walls of the live propellant specimens to a set temperature and then measuring the time-dependent progression of the temperature in the core of the propellant as a function of time and then solving the inverse problem of unsteady state heat transfer to determine the best fit value of the thermal diffusivity. Knowing the values of the density and the specific heat capacity of the propellant, the thermal conductivity of the propellant could be determined at various temperatures. The typical data collected and the solution of the inverse problem to determine the thermal conductivity and the diffusivity are shown in Figure 4. The solution of the inverse problem is adequate and the reproducibility of the results is acceptable. The thermal data can be summarized as:

Density: 1310 kg/m^3

Thermal conductivity: 0.0865 J/(s-m-K)

Specific heat capacity: 1300 J/(kg-K)

The resulting thermal diffusivity is around 5.1E-8 m^2/s. This thermal diffusivity is a relatively small value and indicates that the live propellant is also an insulating material, which makes it rather difficult to cool or heat the propellant in the extruder. This is again seen clearly upon the comparison of the thermal properties of propellant with those of other insulating materials. For example, typical insulating polymers and rubbers have thermal diffusivity values in the range of 5E-8 to 1.5E-7 m^2/s.

Rheological characterization of the double base propellant:

The rheological characterization of a double base propellant is a challenging task. This stems first from the presence of nitrocellulose, NC, fibers. The NC forms a gel with the solvent and plasticizer used in the formulation. The gel exhibits significant wall slip and various types of structuring effects. Data were collected using various types of rheometers. Some of the results are presented here.

Some of the capillary flow data collected using capillaries with the same length over the diameter ratio but at three diameters of 5, 8 and 9 mm and at 77°C (170 °F) are shown in Figure 5. On the basis of apparent slip arguments the shear stress values at the greater diameter should be higher, and this is indeed the case. The shear stress values for the 5 mm die are the smallest following the expected trend.

The wall slip velocity versus the shear stress behavior was characterized as shown in Figure 6. The behavior follows closely the Navier's slip behavior associated with non-Newtonian binders. The slip coefficient and the exponent were determined to be 8.4 E-14 m/(s-Pa ^2.11) and 2.11, respectively. Upon the utilization of the slip correction the wall shear stress versus the corrected (for Rabinowitsch and wall slip) behavior of the double base propellant was obtained and fitted as shown in Figure 7 at 77°C (170 °F). Thus, at 77°C (170 °F) the yield stress of the propellant is 120,000 Pa, the consistency index, 107,079 Pa-s^n, and the shear rate sensitivity index (Power-law index) n, is 0.29.

FEM Analysis of Capillary Flow: FEM analyses of the flow and heat transfer occurring in the capillaries were also made to check the consistency of the data. The pressure distributions obtained with these simulations are shown in Figures 8 and 9. The pressure drop values determined at various flow rates agreed very closely with the results of the experimental individual runs, summarized in Figure 5.

Extrudate Swell:

The extrudate swell data of the gun propellant were collected using an annular die with an internal diameter of 0.430 inch and outer diameter of 0.902 inch, at barrel temperatures of 77, 82, and 88°C (170, 180 and 190°F, respectively) and various crosshead speeds (ram rates) using a capillary rheometer. This annular die was designed and built for the purpose of collecting extrudate swell data under conditions, which should emulate those likely to affect the development of extrudate swell. During the experiments the outer diameter and internal diameter as well as the web thickness of the extrudates were also measured before and after annealing for 16 hours at 71°C (160°F).

One interesting feature of the experiments was the utilization of a thermal imaging camera for the collection of the actual temperature of the extrudate emerging from the annular die. This is an important capability and eliminates potentially significant errors associated with viscous energy dissipation and other effects, which could alter the temperature of the extrudates. Typical temperature scans are shown in Figures 10 and 11, which were used to determine the true temperature distribution of the strands immediately emerging out of the annular die. For example, upon the analysis of the thermal pictures, it was observed that, the outer wall temperature of the material was approximately 81.3°C (178.5°F) when the barrel temperature was set at 88°C (190°F) as shown in Figure 10. The crosscut picture of this same condition shows some cooling effect as shown in Figure 11. The temperature of the material close to the center is similar to the wall temperature measured during extrusion. As one moves towards the outer wall of the cross cut, the temperature decreases, attributed to the temperature of the bushing of the die. Overall, the thermal data allowed us to get accurate values of the temperature of the propellant at the wall in the annular die.

A schematic drawing of the extrudate diameter and thickness swell are provided in Figure 12. The diameter swell and the thickness swell value of the extrudates were calculated with equations provided in the same figure. For the thickness swell the measurements included the direct measurement of the web thickness (the wall thickness) and individual measurements of the inner and the outer diameter of the extrudates, from which again a thickness swell value could be determined.

The diameter and thickness swell values of the extruded strands in various runs are shown in Figures 13 and 14 together with the processing data. The diameter swell value upon averaging for all four conditions is 1.034. There seems to be slight increase in the die swell with increasing extrusion rate, which can be attributed to the reduced residence and increased shear rate at the wall. The magnitude of die swell after annealing was slightly higher than the die swell prior to annealing except for the highest ram rate. The overall range was 1.021 to 1.046. The data were used upon being converted to the extrudate swell versus wall shear stress at various temperatures.

The thickness swell obtained based on the difference of the internal and external diameters again show an increase with increasing shear rate at the wall. The thickness swell based on the direct wall thickness measurements has more scatter. The average thickness swell was 1.10 and was about the same for different methods before and after annealing. The swell data collected in these experiments were used in the sizing of the die used in conjunction with the twin screw extruder.

FEM Analysis of the coupled flow and heat transfer at the continuous processor:

The coupled flow and heat transfer occurring in the twin screw extruder and the die were simulated using an in-house developed Finite Element Method based mathematical model of the die flow and the twin screw extrusion process, based on the direct solution of the conservation equations. The flow geometries did not need to be simplified and FEM meshes were built directly out of the geometrical parameters, which were then varied to obtain the optimum flow channels, which became the basis for the subsequent tool designs. Typical cross-sectional distributions of various parameters at the exit plane of the die are shown in Figures 15-18. The z-velocity distribution (velocity component normal to the cross-sectional plane of the die) indicates that the material moves close to a plug except at the wall areas, which exhibit very small velocities and hence will generate relatively long residence times. The exact value of the residence time of the material moving adjacent to the die wall is governed by the adhesive characteristics of the propellant and its wall slip behavior. The maximum stress magnitude is found at the walls of the die and is restricted to about 233 KPa (Figure 16). The shear rate distribution (the second invariant of the rate of deformation tensor) is shown in Figure 17 and the maximum at the wall is at 0.9 s^{-1}. This is a relatively very small value and suggests that the viscous energy dissipation effects in the straight land section of the die will be negligible. The resulting temperature distribution in the emerging grain reflects this and the temperature distribution is basically governed by the heat transfer through the wall of the die (Figure 18). In these calculations the stake surface is kept under adiabatic conditions and thus the actual temperature distribution is likely to be more uniform than what is presented here.

Overall, such FEM results enabled the determination of the optimum flow geometries as well as the prediction of safe conditions for the twin screw extrusion of the propellant.

Conclusions

A combination of experimental characterization methods and numerical simulation techniques were applied to develop the engineering base for the twin screw extrusion of a double base formulation. The use of such detailed analysis methods prior to the extrusion of the first pound of the live propellant provides a rigorous assessment of the thermo-mechanical conditions that the propellant will experience in the twin screw extruder and the die, allow the design of the die for net-shape extrusion of the propellant grain to reduce subsequent labor, provide a first order safety analysis on the process and generate the optimum conditions and geometries/designs for the twin screw extrusion process.

Acknowledgements

This project was funded by the ESTCP (Environmental Security Technology Certification Program) under Project #199804. We are grateful for this funding which made this study possible. We thank Ms. Constance Murphy and Mr. John Brough for their helpful input and encouragement.

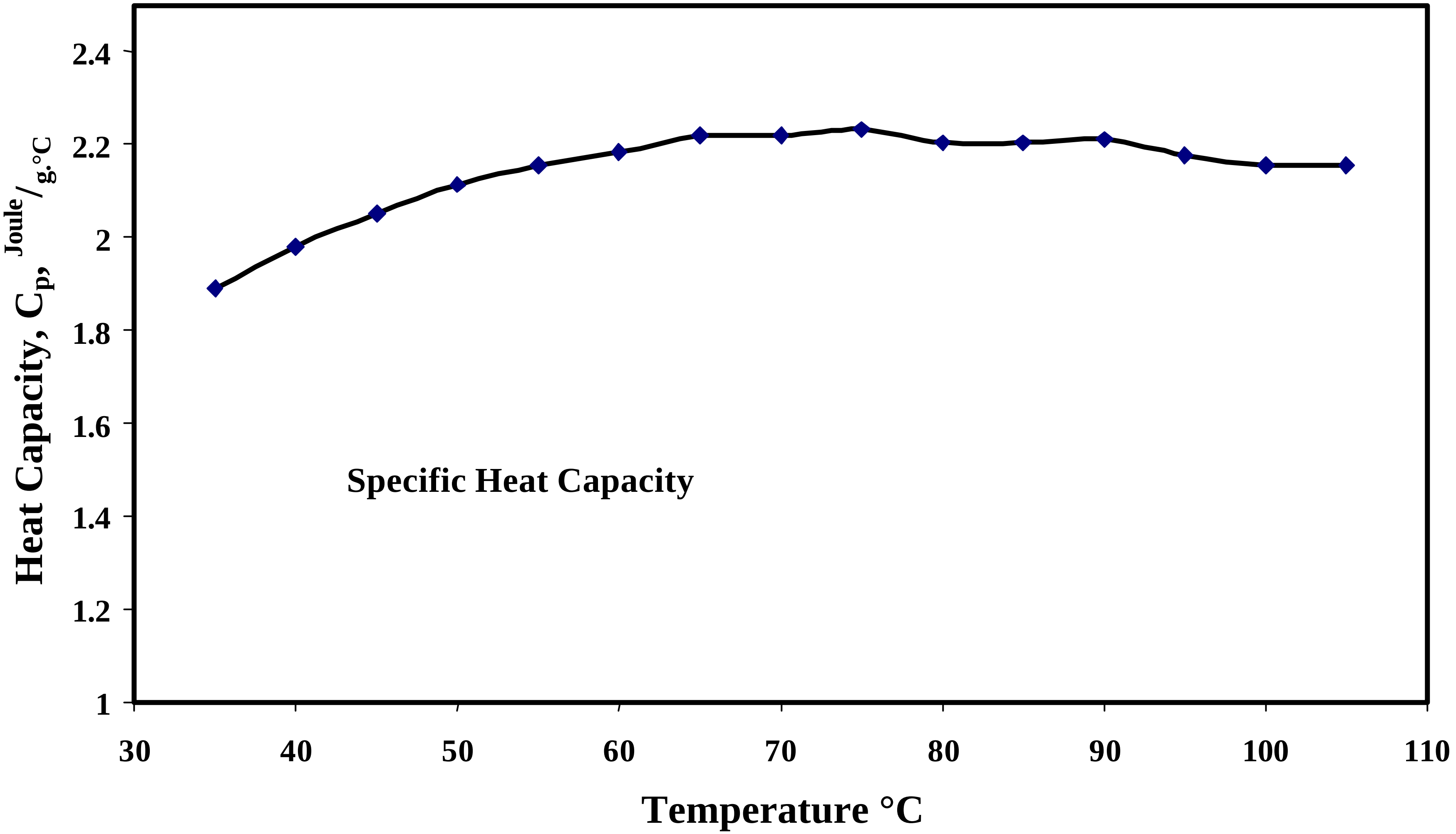

Heat Capacity, Cp, Joule/g.°C
2.4
2.2
2
1.8
1.6
1.4
1.2
1
Specific Heat Capacity
30
40
50
60
70
80
90
100
110
Temperature °C

Figure 1

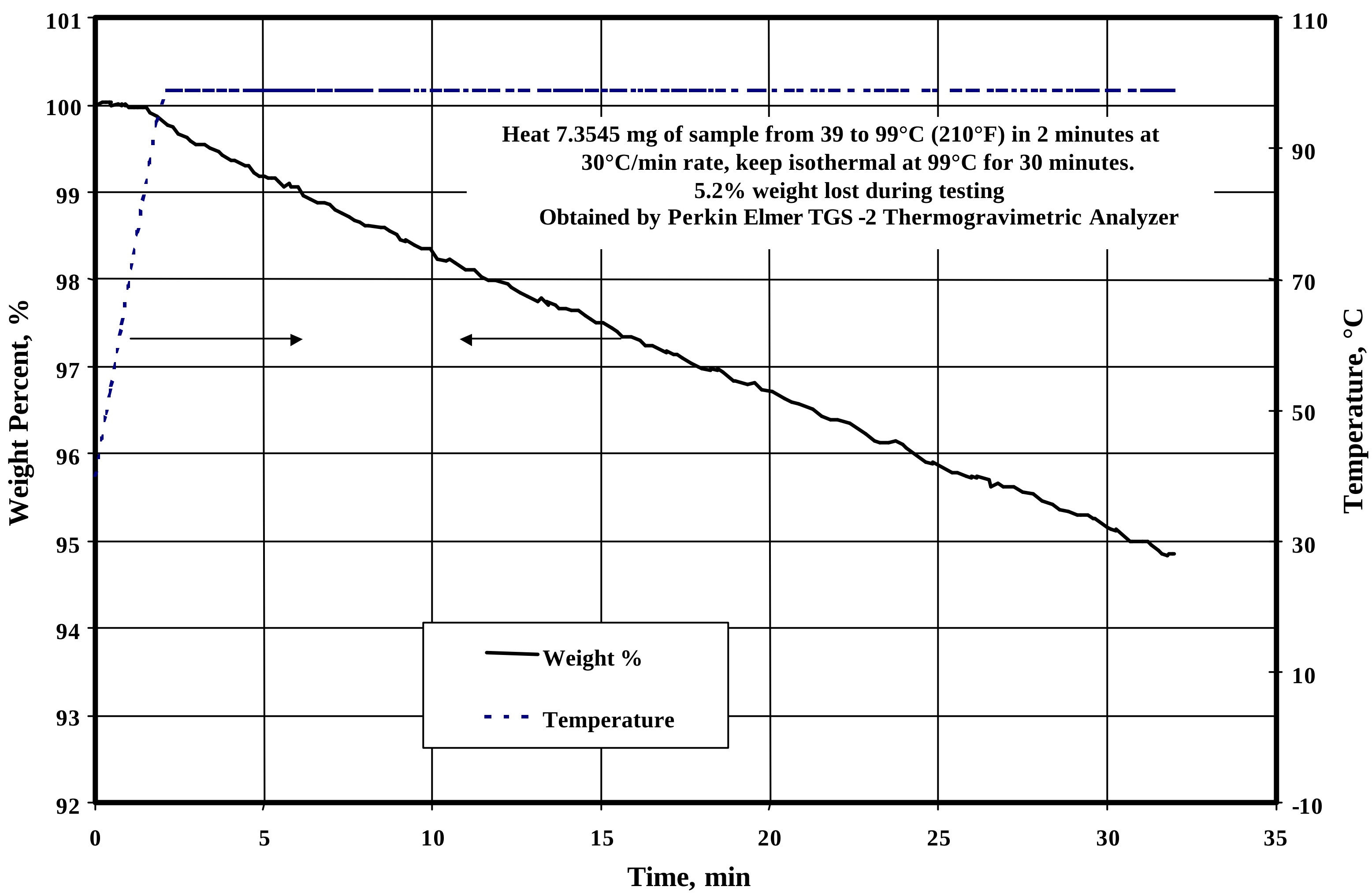

Heat 7.3545 mg of sample from 39 to 99°C (210°F) in 2 minutes at 30°C/min rate, keep isothermal at 99°C for 30 minutes.
5.2% weight lost during testing
Obtained by Perkin Elmer TGS -2 Thermogravimetric Analyzer
Weight %
Temperature
Weight Percent, %
Temperature, °C
Time, min
101
100
99
98
97
96
95
94
93
92
110
90
70
50
30
10
-10
0
5
10
15
20
25
30
35

Figure 2

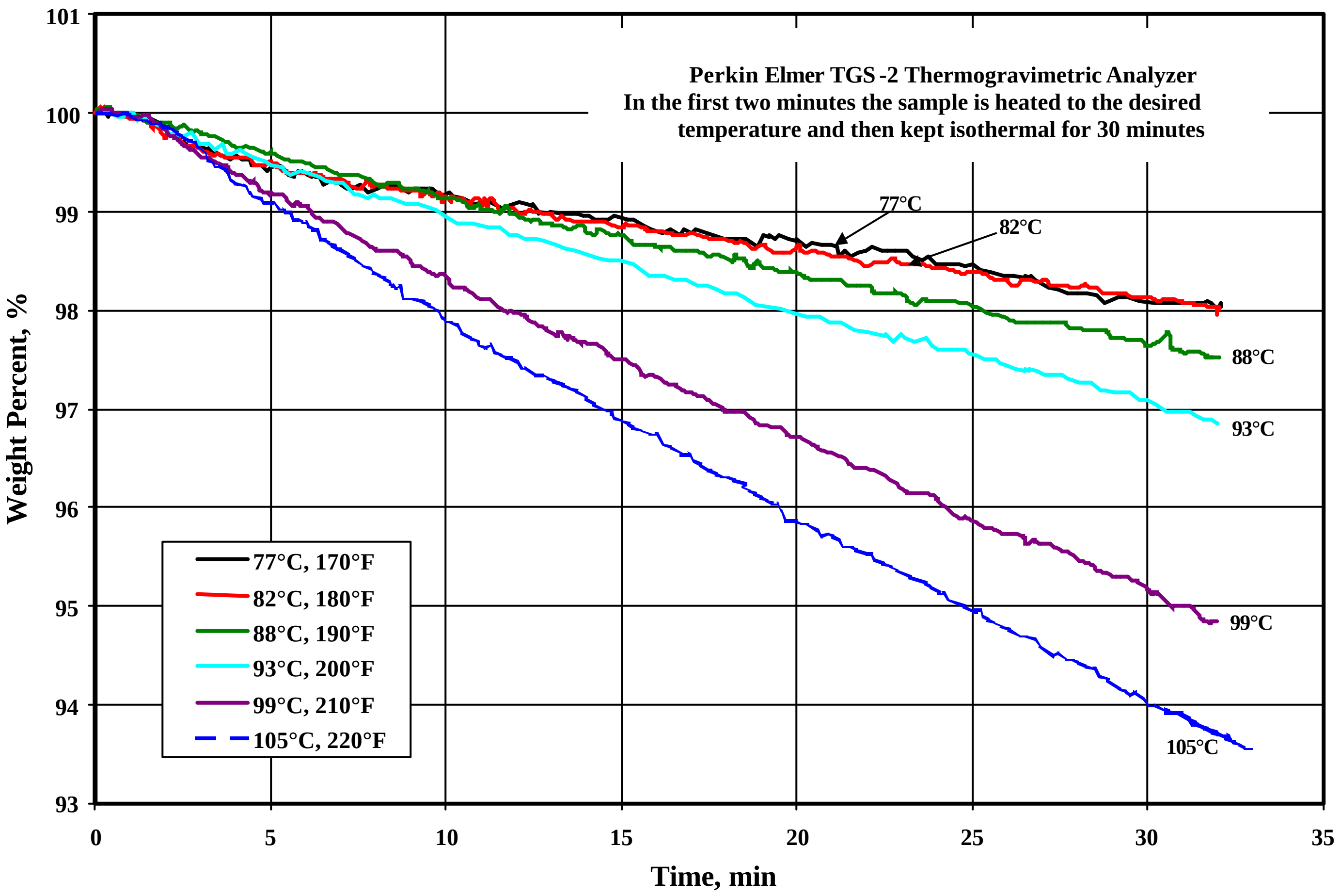
Perkin Elmer TGS-2 Thermogravimetric Analyzer
In the first two minutes the sample is heated to the desired temperature and then kept isothermal for 30 minutes
Weight Percent, %
Time, min
101
100
99
98
97
96
95
94
93
0
5
10
15
20
25
30
35
77°C
82°C
88°C
93°C
99°C
105°C
77°C, 170°F
82°C, 180°F
88°C, 190°F
93°C, 200°F
99°C, 210°F
105°C, 220°F

Figure 3

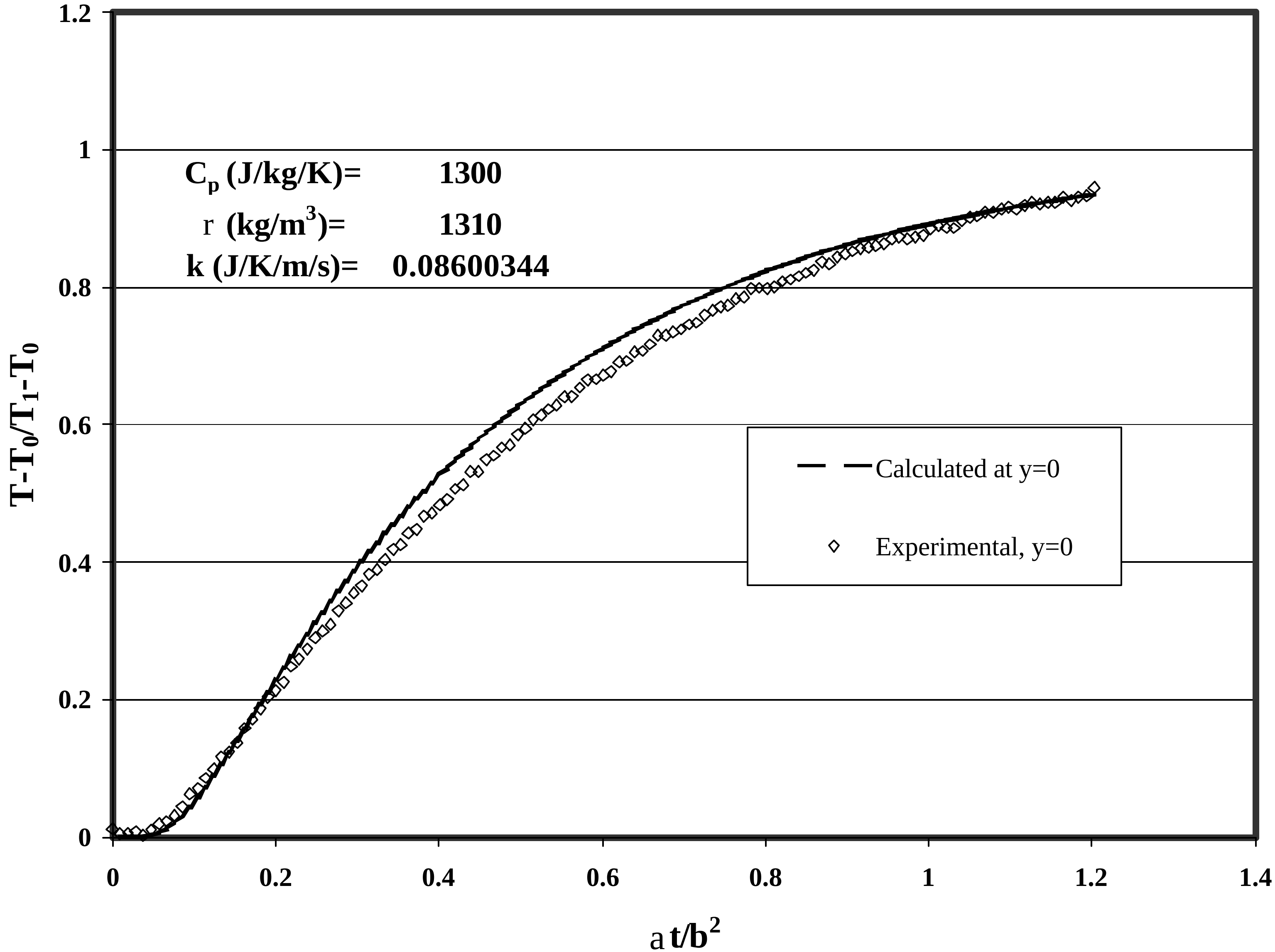

Live double base rocket propellant:
Thermal Diffusivity determination

Figure 4

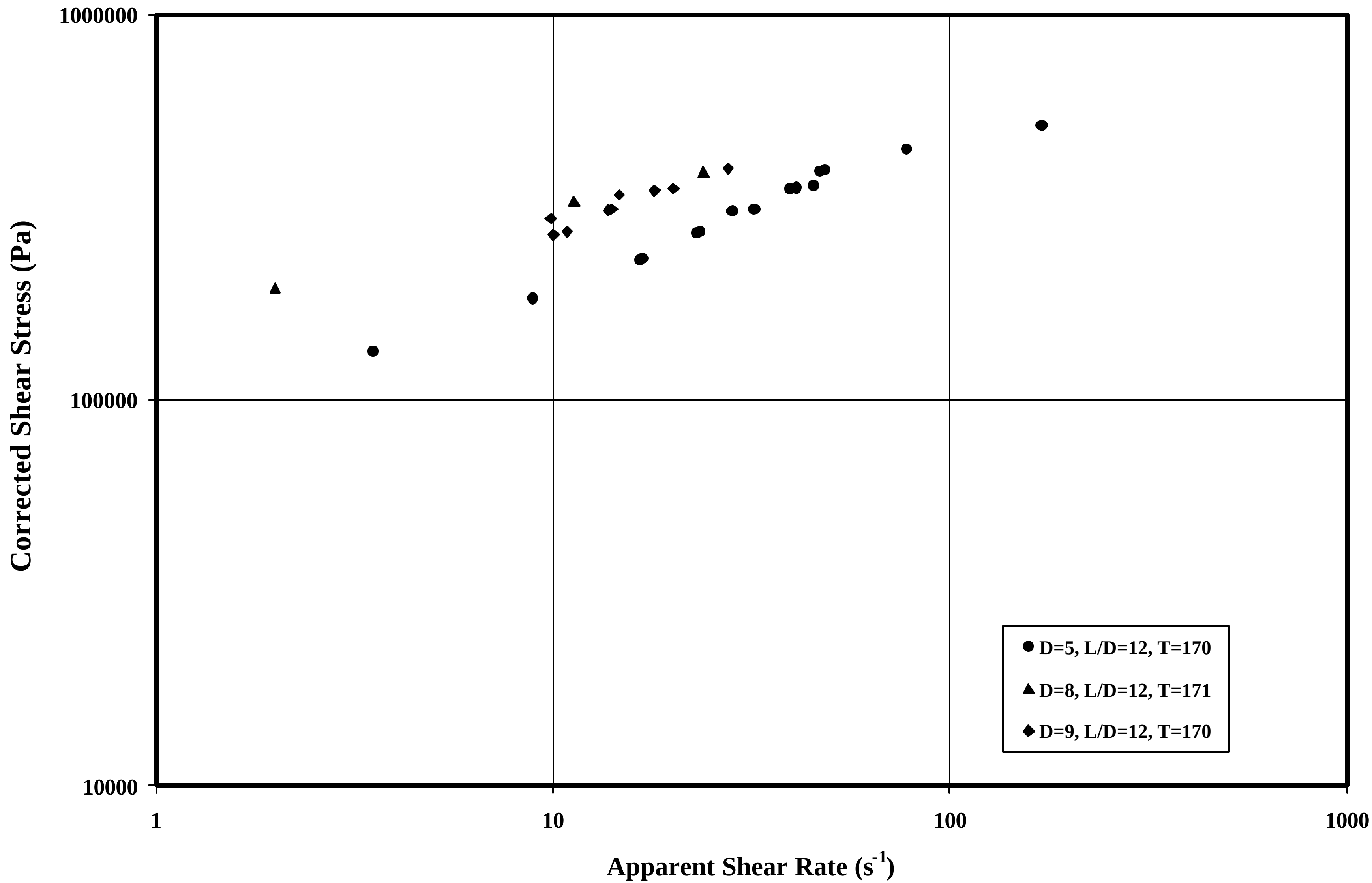

Surface/volume ratio dependence of the flow curves:

at 77 °C (170 °F).

Figure 5

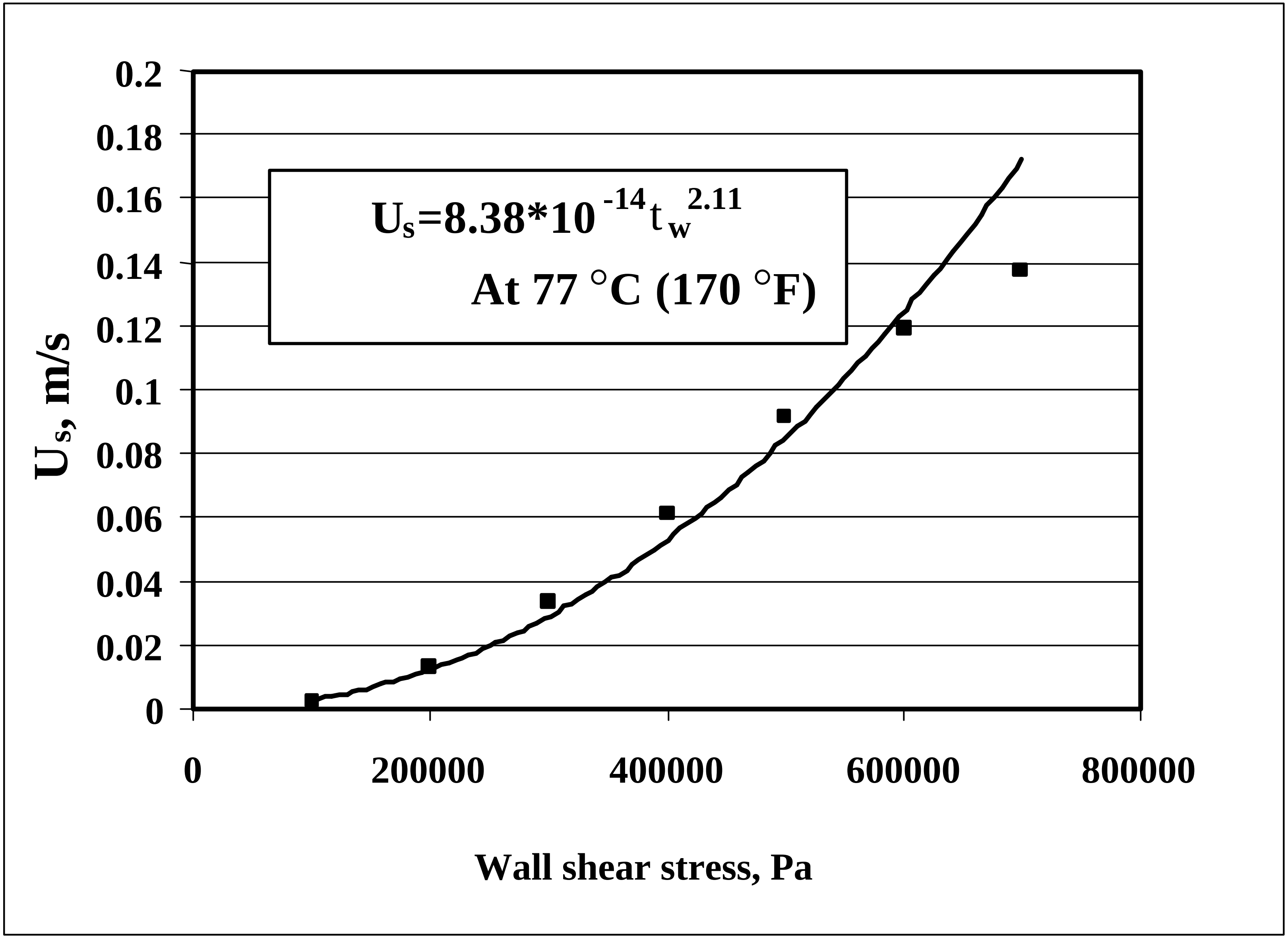

Slip velocity, U_s, versus the wall shear stress at 77 °C (170 °F).

Figure 6

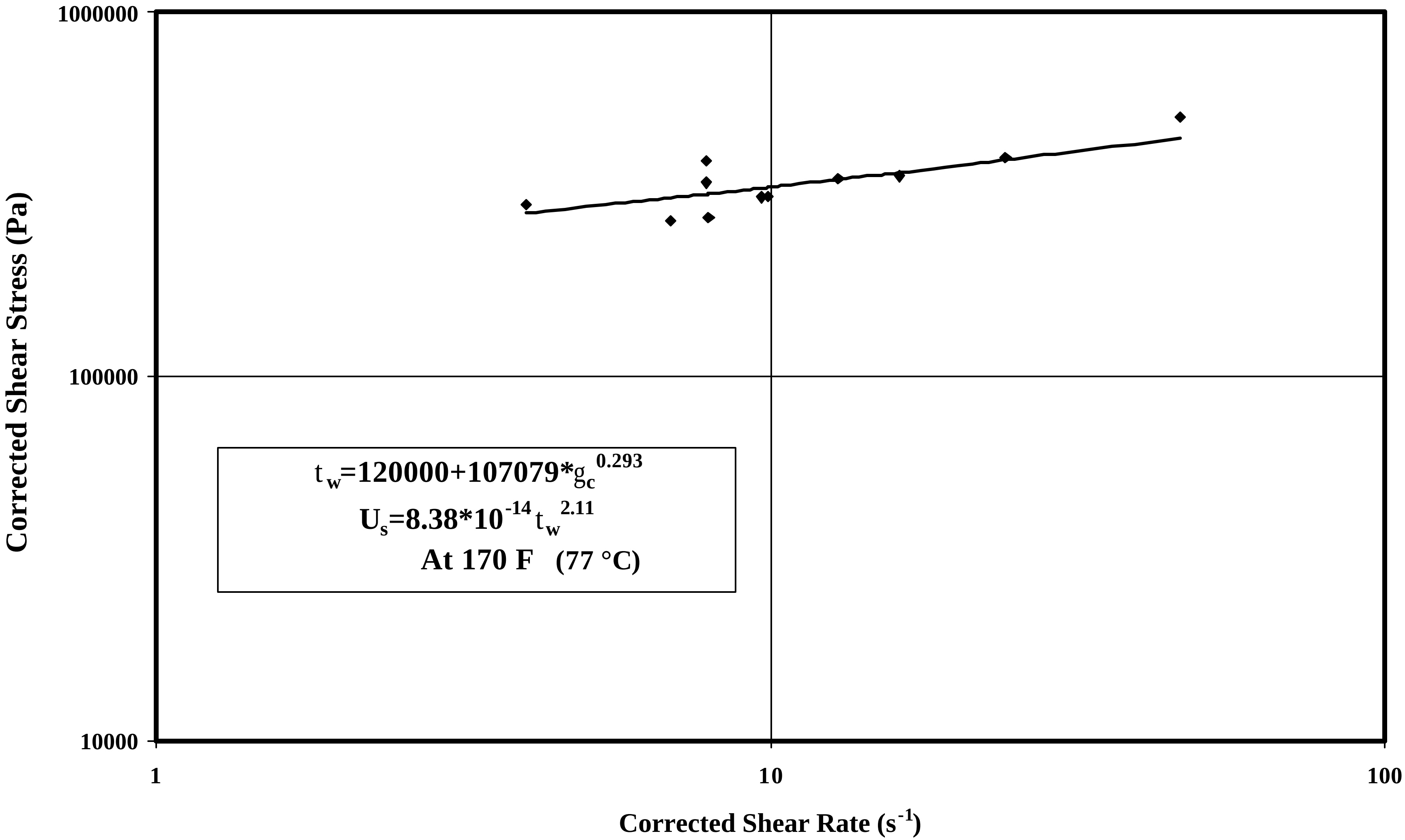

Slip corrected data together with Rabinowitsch correction

Figure 7

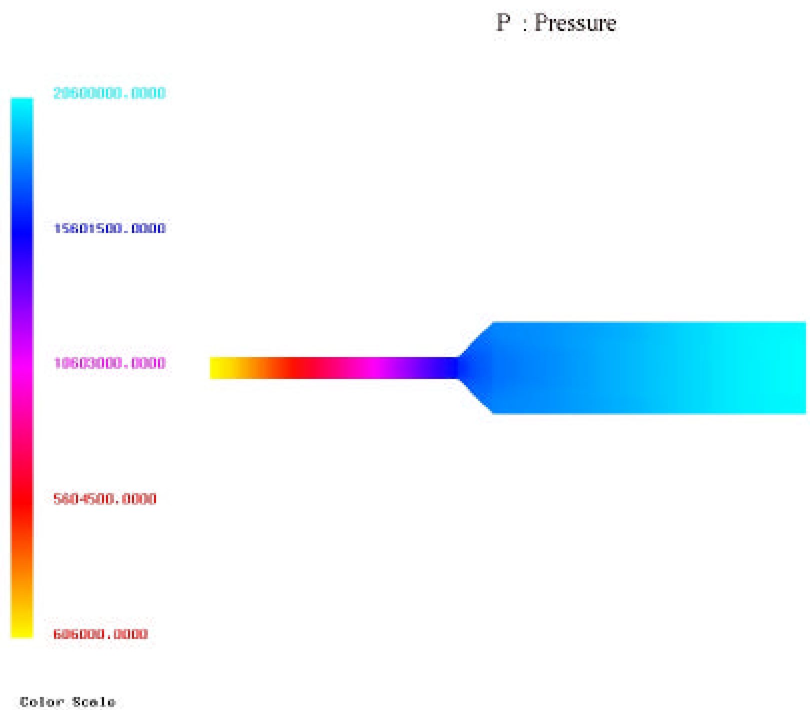

0.27 kg/hr (0.6 lb/hr) at 77 °C (170 °F) with 5 mm capillary with L/D=12

Figure 8

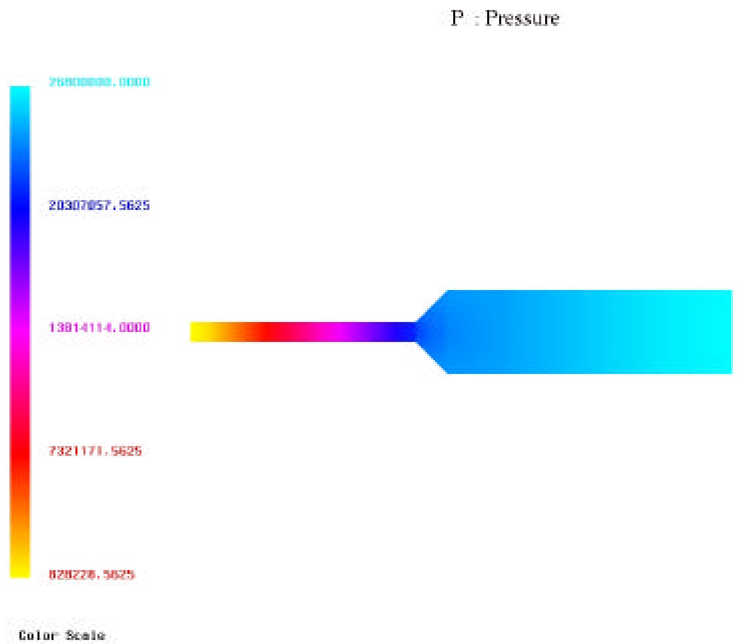

1.95 kg/hr (4.3 lb/hr) at 77 °C (170 °F) with 5 mm capillary with L/D=12

Figure 9

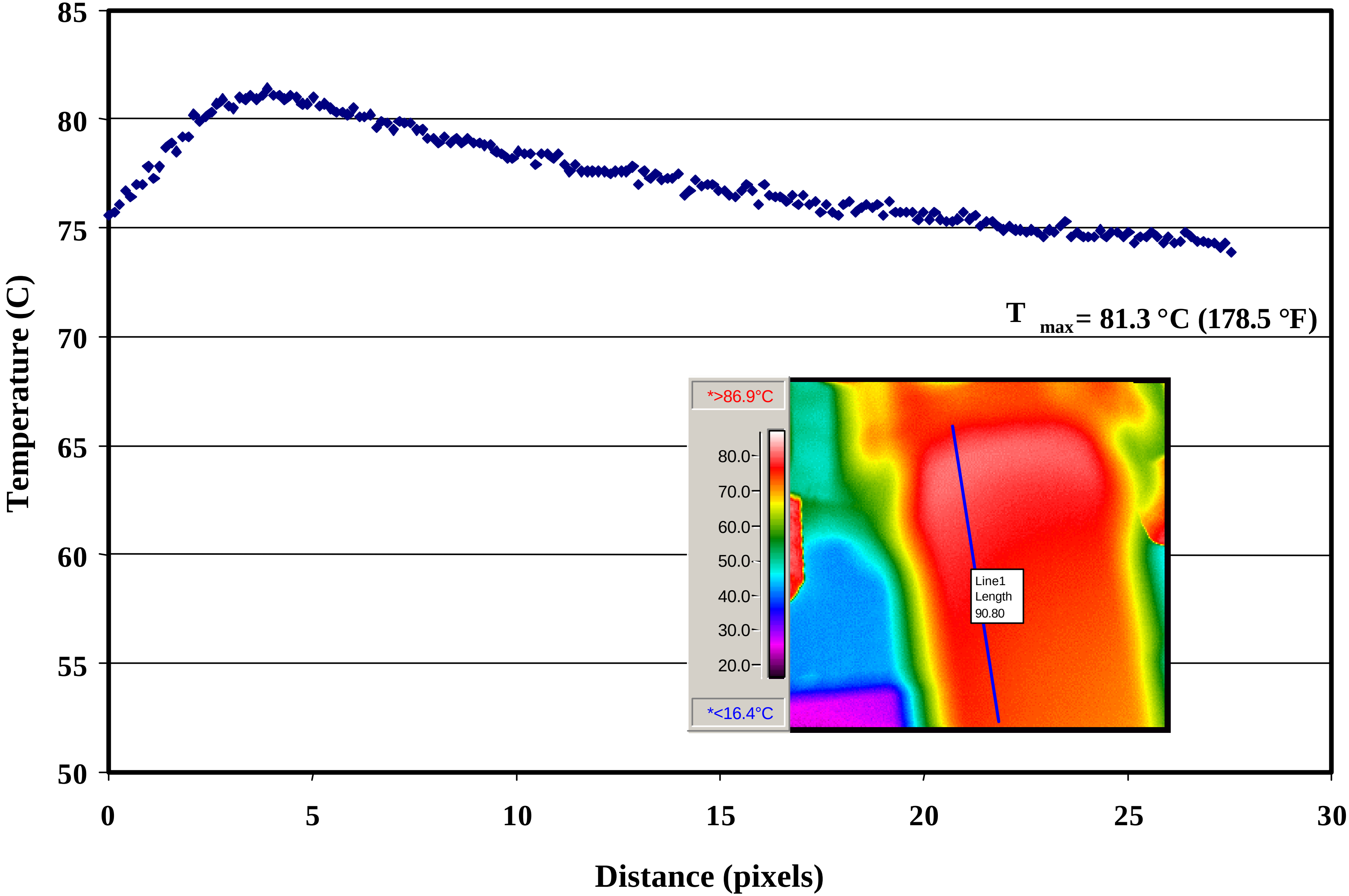
85
80
75
70
65
60
55
50
Temperature (C)
0
5
10
15
20
25
30
Distance (pixels)
T max= 81.3 °C (178.5 °F)
*>86.9°C
80.0
70.0
60.0
50.0
40.0
30.0
20.0
*<16.4°C
Line1
Length
90.80

Figure 10

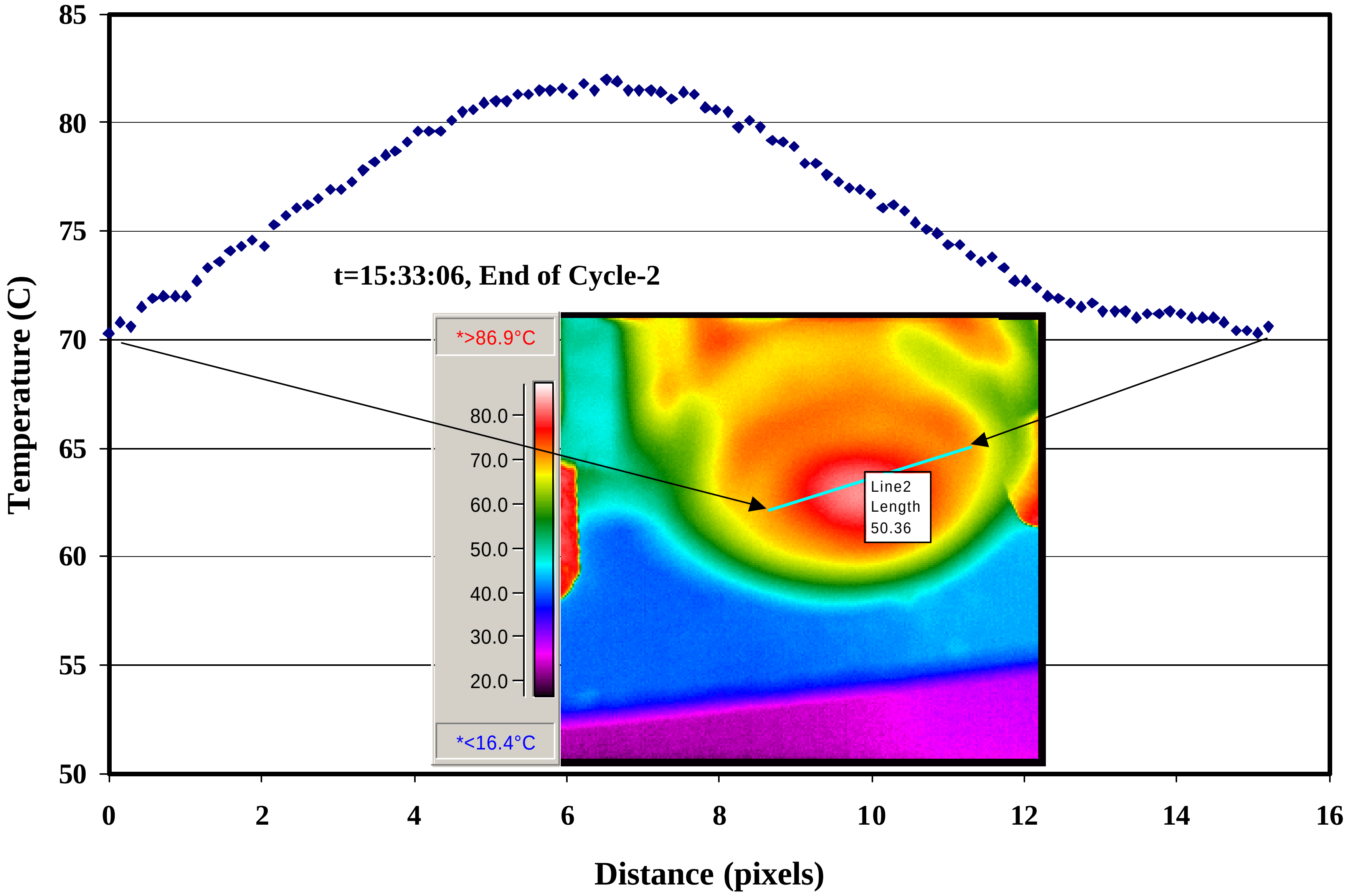
85
80
75
70
65
60
55
50
Temperature (C)
0
2
4
6
8
10
12
14
16
Distance (pixels)
t=15:33:06, End of Cycle-2
*>86.9°C
80.0
70.0
60.0
50.0
40.0
30.0
20.0
*<16.4°C
Line2
Length
50.36

Figure 11

$$S_D = \frac{D_0}{D_2}$$

$$S_{T\ OD-ID} = \frac{D_0 - D_i}{D_2 - D_1}$$

$$S_{T\ Web} = \frac{Web}{\frac{D_2 - D_1}{2}}$$

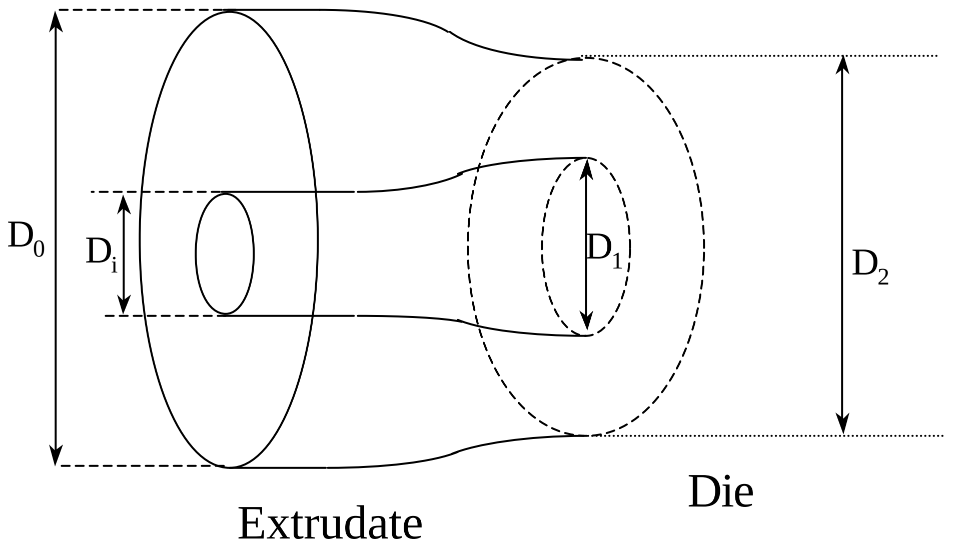

Figure 12

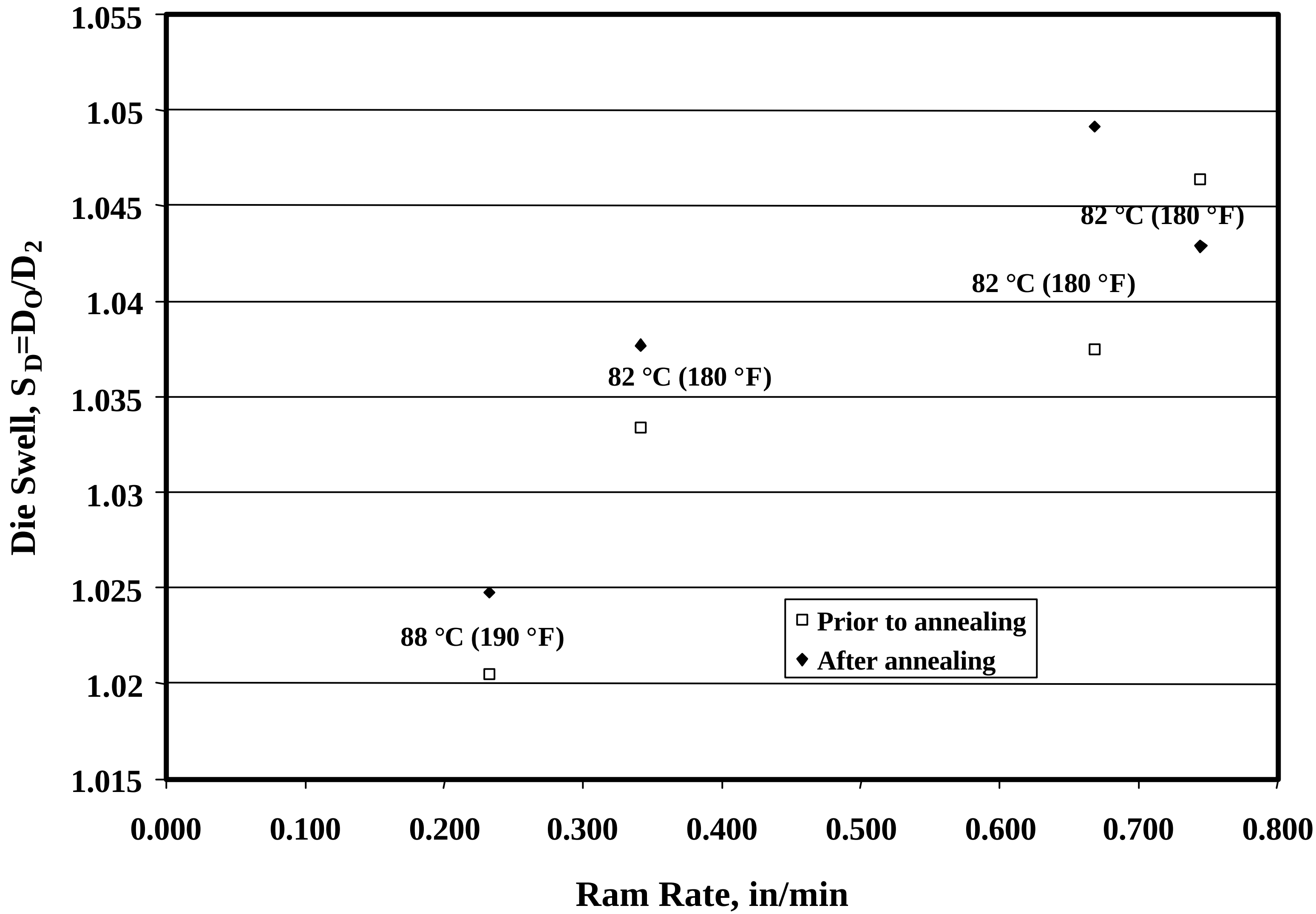

1.055
1.05
1.045
1.04
1.035
1.03
1.025
1.02
1.015
Die Swell, S_D=D_O/D_2
0.000
0.100
0.200
0.300
0.400
0.500
0.600
0.700
0.800
Ram Rate, in/min
82 °C (180 °F)
82 °C (180 °F)
82 °C (180 °F)
88 °C (190 °F)
Prior to annealing
After annealing

Figure 13

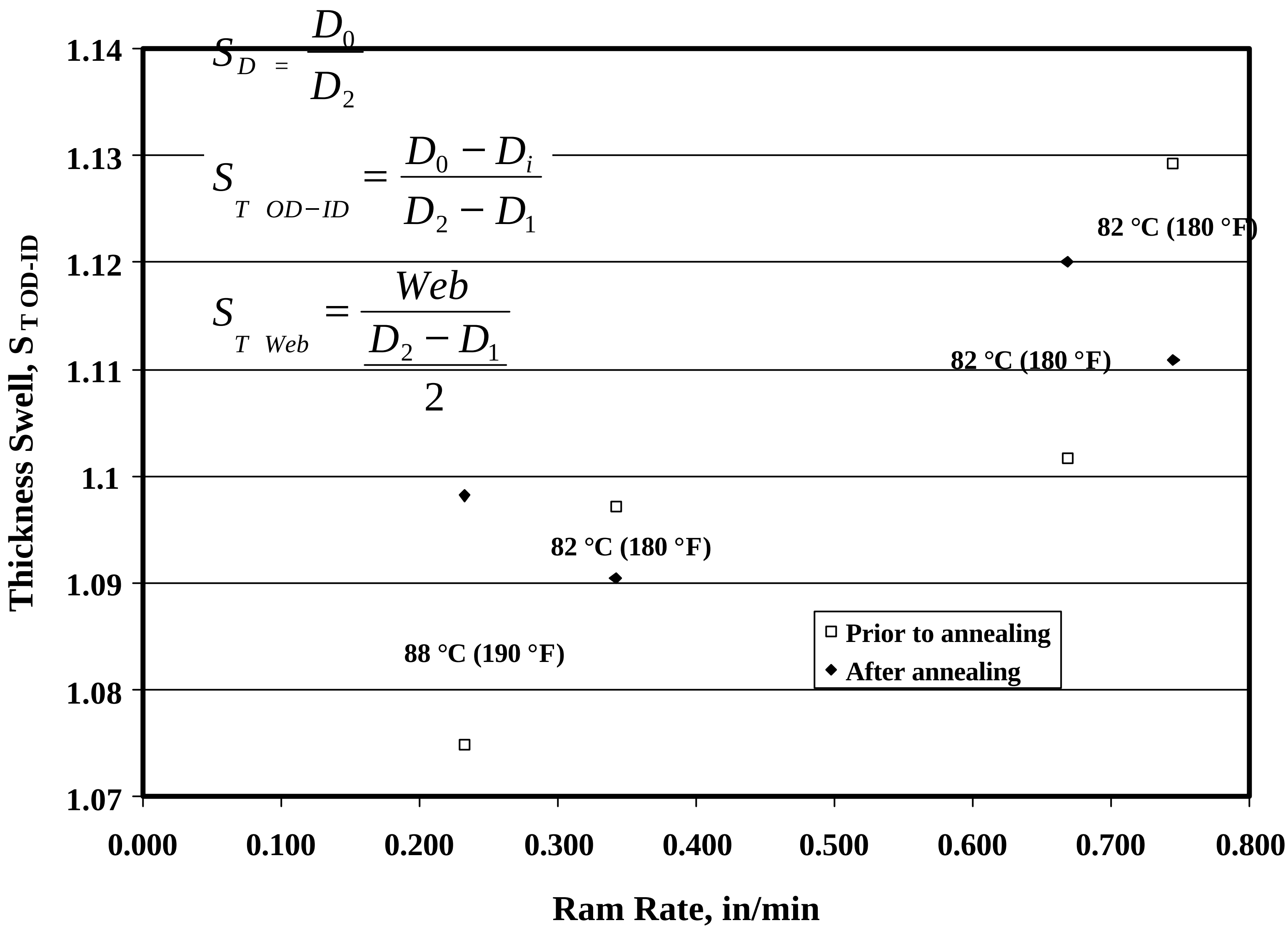

$S_D = \frac{D_0}{D_2}$
$S_{T\ OD-ID} = \frac{D_0 - D_i}{D_2 - D_1}$
$S_{T\ Web} = \frac{Web}{\frac{D_2 - D_1}{2}}$
82 °C (180 °F)
82 °C (180 °F)
82 °C (180 °F)
88 °C (190 °F)
Prior to annealing
After annealing
1.14
1.13
1.12
1.11
1.1
1.09
1.08
1.07
0.000
0.100
0.200
0.300
0.400
0.500
0.600
0.700
0.800
Ram Rate, in/min
Thickness Swell, $S_{T\ OD\text{-}ID}$

Figure 14

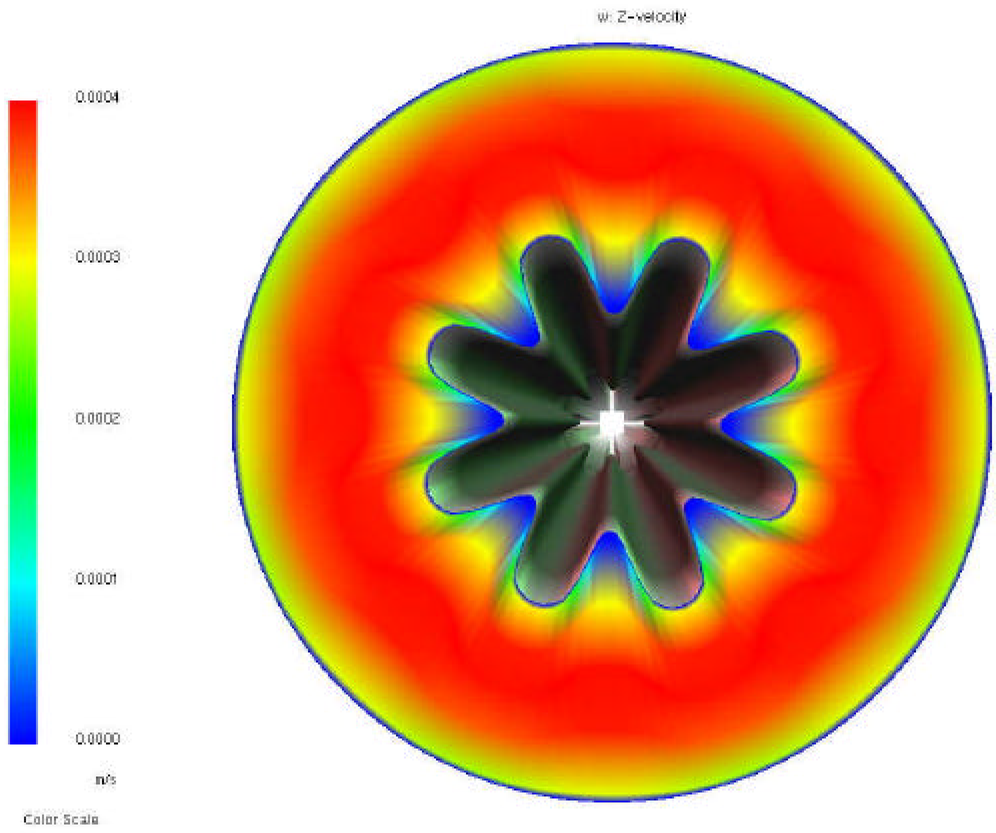

z-velocity distribution at 4.5 kg/hr (10 lb/hr) with the die bushing wall at 77 ° C (170 °F)

Figure 15

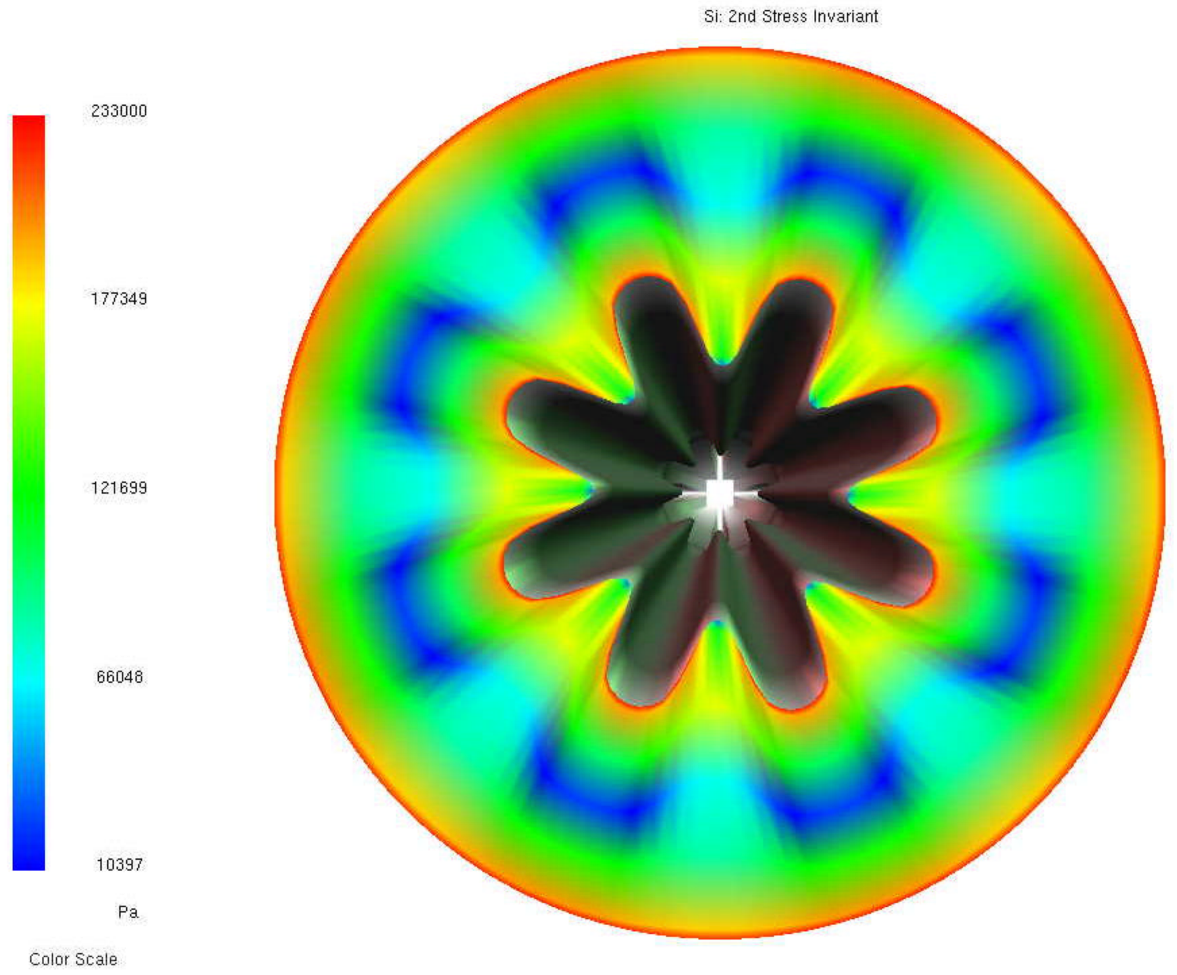

Stress magnitude distribution 4.5 kg/hr (10 lb/hr) with the die bushing wall at 77 °C (170 °F)

Figure 16

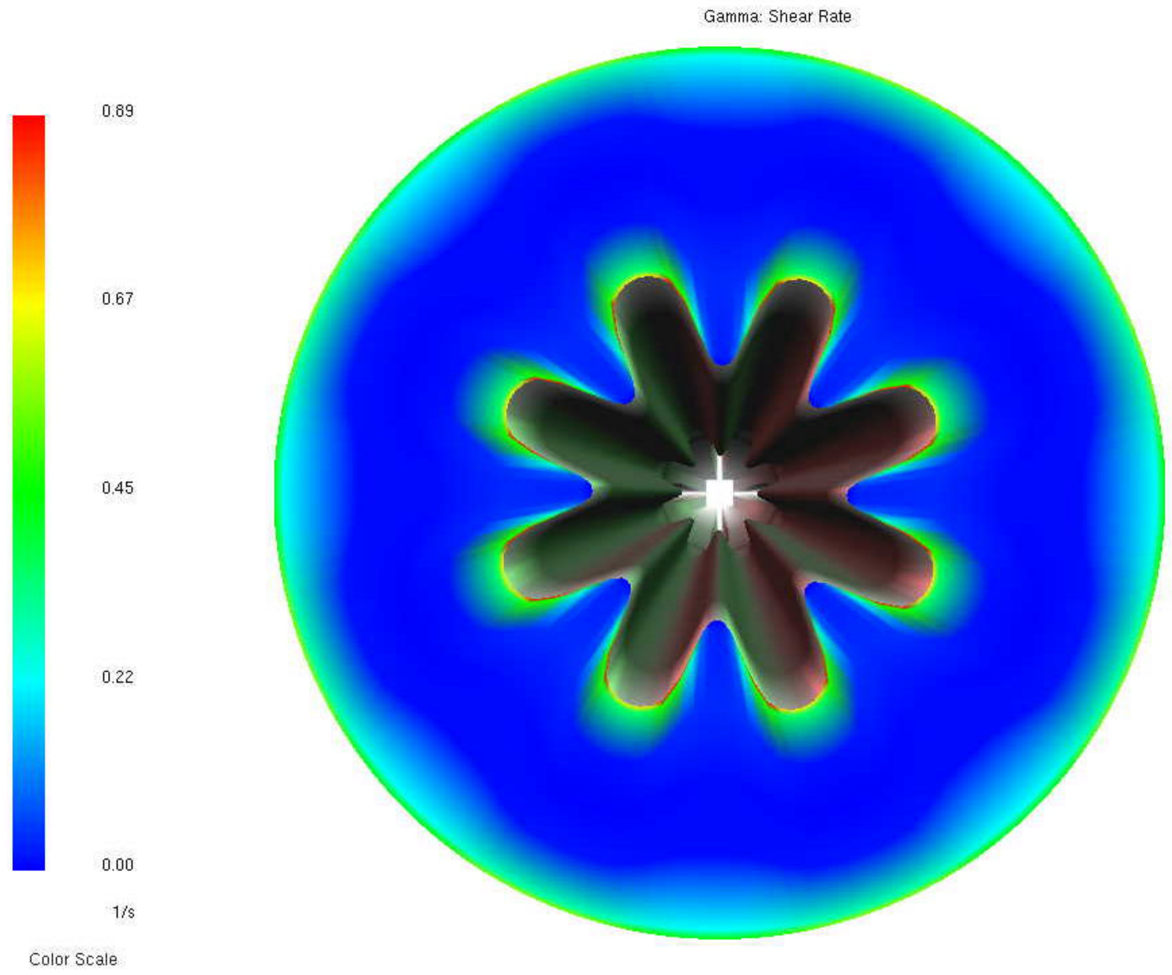

Shear rate (second invariant of the deformation rate tensor) distribution at
4.5 kg/hr (10 lb/hr)
with the die bushing wall at 77 ° C (170 °F)

Figure 17

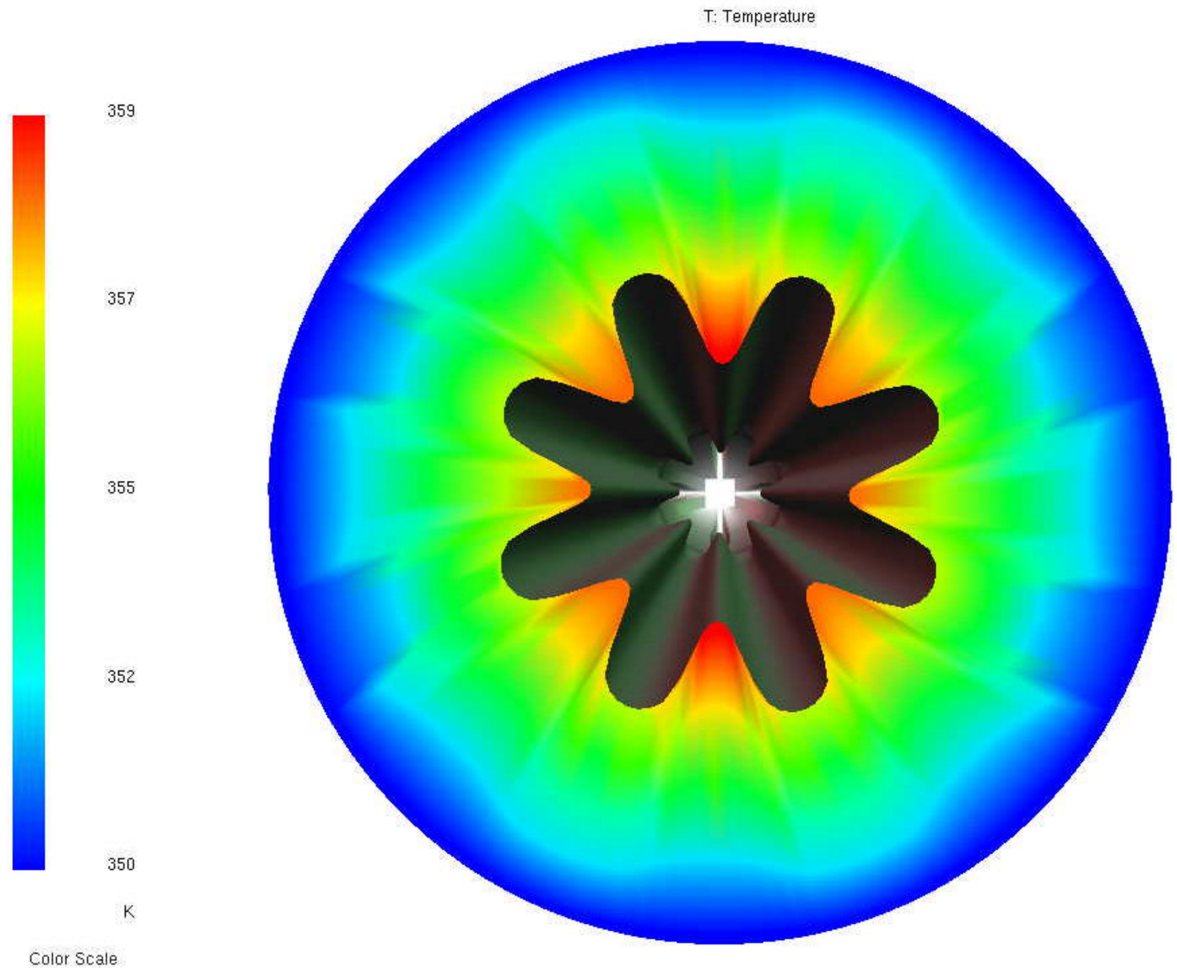

Temperature distribution at 4.5 kg/hr (10 lb/hr) with the die bushing wall at 77 ° C (170 °F) and with the mandrel assumed to be adiabatic.

Figure 18